Velocity distribution of CO desorbing from NiO(100)/Ni(100) after picosecond UV laser irradiation

B. Redlich [a], A. Kirilyuk [b], T. Hoger [c], G. von Helden [d], G. Meijer [d], H. Zacharias [c,*]

[a] *FOM Institute for Plasma Physics, "Rijnhuizen", Nieuwegein, 3439 MN, Netherlands*
[b] *Research Institute for Materials, University of Nijmegen, 6525 ED Nijmegen, Netherlands*
[c] *Physikalisches Institut, Westfälische Wilhelms-Universität, 48149 Münster, Germany*
[d] *Fritz-Haber-Institut der Max-Planck-Gesellschaft, 14195 Berlin, Germany*

Abstract

The UV laser-induced desorption of CO from an epitaxial film of NiO(100) on Ni(100) yields a linear dependence of the desorption signal on the laser intensity with a cross-section of $(8.3 \pm 0.9) \times 10^{-18} \, \mathrm{cm^2}$. Rotational and vibrational temperatures of 870 K and 1340 K, respectively, are observed. State-resolved velocity distributions are observed, where one part can be described by a Maxwellian flux distribution with $\langle E_{kin} \rangle / 2k$ ranging from 1000 to 1800 K. In addition a faster component is present which gains in importance for increasing J''. A distinct rotation–translational coupling is found.
© 2005 Elsevier B.V. All rights reserved.

1. Introduction

The understanding of photochemical processes and reactions at solid surfaces is of fundamental importance, as well as of practical relevance for a variety of processes like heterogeneous photocatalysis or photochemical processes and for the micro and nano structuring of surfaces. For molecules adsorbed on metallic substrates detailed studies have been performed with a variety of adsorbates, substrates and photon energies [1]. It is commonly accepted that on these surfaces photoexcitation of the electronic system of the metal constitutes the primary process. Besides energy dissipation to the bulk scattering of the hot electrons at the adsorbate generates vibrational and electronic excitations which after coupling to the desorption coordinate eventually lead to desorption of the adsorbate.

Similar studies on insulating substrates with large band gaps remain comparatively sparse. In this case the creation of a gas of hot electrons with a broad energy distribution may no longer be the dominant excitation pathway of

adsorbed molecules. At photon energies above the band gap, substrate electronic excitations to the conduction band, thereby creating electron–hole pairs, followed by rapid intraband relaxation to the bottom of this band constitutes an excitation scheme similar to that proposed for metal substrates. For physisorbed molecules direct excitations like in the gas phase are possible, and for chemisorbed adsorbates also direct optical transitions from the substrate to electronically excited states of the adsorbate/substrate complex may be considered.

On oxide surfaces earlier experiments using nanosecond UV laser radiation have been carried out for NO desorption from NiO(100) [2,3] and $Cr_2O_3(0001)$ [4]. Femtosecond laser excitations have concentrated on NO desorption from NiO(100) [5]. On these surfaces NO adsorbs in a bent geometry [6,7], while in an electronically excited NO^- configuration the equilibrium geometry is upright [8–10]. Carbon monoxide on the other hand adsorbes in the ground state in nearly linear configuration ($\vartheta \sim 7°$) [11–14] and for electronically excited CO a bent geometry is expected. Experimental studies for laser-induced CO desorption have been performed mostly for metal substrates [15–19] using femtosecond laserpulses. Nanosecond UV laser desorption

---

* Corresponding author.
   E-mail address: hzach@uni-muenster.de (H. Zacharias).

of CO has been performed for $Cr_2O_3(0001)$ [20–22] and NiO(111) [23] substrates. The latter surface differs from the one investigated in the present study in that the polar NiO(111) surface exhibits terraces with either pure Ni or pure O termination, while NiO(100) is terminated by a neutral-Ni–O-configuration.

2. Experimental

The experiment is performed in an ultrahigh vacuum (UHV) chamber with a base pressure of less than 2×10^{-10} mbar. Surface structure and cleanliness are controlled with LEED and Auger electron spectroscopy. Cleaning of the sample is accomplished by Ar ion bombardment at low kinetic energy. The epitaxial film of NiO(100) is prepared by repeated cycles of oxidation with O_2 at pressures up to 5×10^{-6} mbar and annealing at temperatures between 570 and 700 K [7]. The sample can be cooled down to 110 K and heated up to 1000 K. The initial preparation of the CO adsorbate layer occurs via background dosing at 110 K. At this temperature about half a monolayer of CO can be adsorbed on the NiO(100) thin film [24]. For redosing between the desorption laser pulses a pulsed valve is employed to keep a steady state coverage of carbon monoxide.

The desorption of the CO molecules is initiated by the radiation of a frequency quadrupled Nd:YAG laser at $\lambda = 266$ nm ($h\nu = 4.66$ eV) with a pulse duration of 80 ps and operating at 5 Hz repetition rate. The p-polarized radiation was incident under 45° with respect to the surface normal. Pulse energies up to 1.9 mJ are applied to a spot size of about 10 mm^2 area, resulting in fluences of up to 19 mJ/cm^2.

The desorbed CO molecules are detected rovibrational state selectively by resonance enhanced multiphoton ionisation (2 + 1 REMPI) via the B $^1\Sigma^+(v' = 0,1) \leftarrow$ X $^1\Sigma^+(v'' = 0,1)$ transition [25]. The generated photoions are measured by microchannel plates. Although this detection scheme suffers from an unresolved Q-branch at low J'' it was chosen, because it avoids problems which might be caused by a possible strongly varying rotational alignment as was observed for desorption from $Cr_2O_3(0001)$ [21]. The tuneable ($\lambda \sim 230$ nm) probe laser radiation with a line width of ~ 0.21 cm^{-1} is provided by a frequency doubled dye laser pumped by the third harmonic of a Q-switched Nd:YAG laser. Operating at 10 Hz repetition rate UV pulse energies of 100 µJ with 8 ns duration are applied. The probe laser beam has a diameter of 0.1 mm and a two-photon Rayleigh length of 44 mm. It intersected the desorption flux at a distance of 20 mm in front of the surface. No attempt has been made to restrict the polar angle of detection, exciting thus desorbing molecules in an angular range of ± 45°. Operating the electronics in a toggle mode enabled an efficient registration of background CO molecules from the gas phase between desorption laser pulses. At the probe laser intensity applied the B–X two-photon transition of CO is not saturated, thus the

Hönl–London factors have to be taken into account. However, since we are only detecting Q-branch transitions, the Hönl–London factors for a $^1\Sigma$–$^1\Sigma$ transition are independent of the rotational quantum number [26]. By varying the time delay between desorption and probe laser pulses information about the kinetic energies of the desorbing molecules is obtained.

3. Results and discussion

The desorption yield increases linearly with laser intensity up to a maximum applied pulse energy of 1.9 mJ, which corresponds to a fluence and intensity of 19 mJ/cm^2 and 2×10^{11} W/cm^2, respectively. For such a linear intensity dependence the desorption yield can be expressed by an effective desorption cross-section σ_{des} via

$$\ln(N/N_0) = -\sigma_{des} \times n_{ph}, \tag{1}$$

where N_0, N, n_{ph} denote the number of adsorbate molecules before and after desorption and the photon flux, respectively. The cross-section is related to the photon flux applied to the CO/NiO(100) system. The desorption cross-section has been determined on the rotational Q-branch bandhead of the ($v'' = 0$) state at a probe laser delay time of 25 µs, where the arrival time distribution peaks. Fig. 1 displays the decay of the CO desorption yield. Here the logarithm of the desorption signal is plotted versus the applied photon flux. A strong decrease of the signal is observed up to an accumulated flux of about 1.5×10^{17} photons/cm^2, followed by a more shallow diminution. From the initially strong decrease an effective desorption cross-section of $\sigma_{des} = (8.3 \pm 0.9) \times 10^{-18}$ cm^2 is derived. This channel accounts for more than 80% of the desorption flux. The slower decay at higher total photon flux may be described by a cross-section of $\sigma_{des} = (1.8 \pm 0.2) \times 10^{-18}$ cm^2.

Such a bimodal decay of the coverage is also observed for UV laser induced desorption from NiO(111) at 4 eV
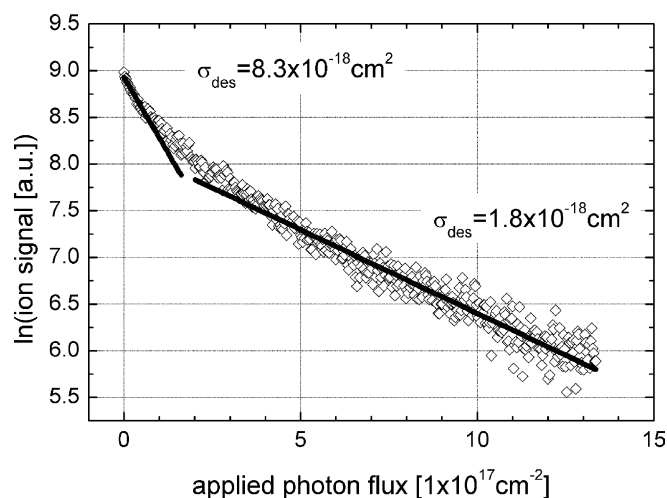

Fig. 1. Semi-logarithmic plot of the desorption yield as a function of applied photon flux.

photon energy [23]. In that experiment cross-sections of 3.3×10^{-18} cm^2 and 4.5×10^{-19} cm^2 for the fast and slow decay, respectively, were measured. Since the ground state binding energy of CO on nickel oxide is higher for the (1 0 0) than for the (1 1 1) surface, the generally higher cross-sections in the present study might be a first hint to a more effective electronic excitation of the system. Similary, the desorption of NO from NiO(1 0 0) shows a bimodal decay [3,5]. While the initial cross-section for CO desorption is lower by a factor of 2.3 than the corresponding one for NO of 1.9×10^{-17} cm^2, the slow decay shows a nearly one order of magnitude higher cross-section (NO: 2.7×10^{-19} cm^2). The slow decay might originate from molecules adsorbed on step and defect sites of the NiO(1 0 0) surface. The cross-section for CO desorption from Cr$_2$O$_3$(0 0 0 1) of 3.5×10^{-17} cm^2 at $\lambda = 193$ nm is significantly larger [20]. According to mechanisms where desorption is induced by an electronic transition to an excited state (DIET) a large desorption cross-section implies a comparatively long lifetime of the electronically excited state, estimated here to be in the range of about 10–30 fs.

Desorbing CO molecules are rotational state selectively detected in both the vibrational ground and the first vibrationally excited state. With the given spectral resolution the Q-branch heads at 230.106 nm and at 230.259 nm of the (0–0) and (1–1) band, respectively, could not be resolved into their rotational components, but for $J'' \geqslant 12$ single rotational states could be addressed. In ($v'' = 0$) rotational states up to $J'' = 37$ and in ($v'' = 1$) rotational states up to $J'' = 22$ are observed. The former limit is given by the threshold to predissociation in the B $^1\Sigma^+$ ($v' = 0$) state which begins at $J' = 38$, while in the B $^1\Sigma^+$ ($v' = 1$) state slow predissociation sets in at $J' = 17$ [27,28]. An abrupt decrease in intensity above the predissociation limits is not observed, since the predissociation rate of about 10^{10} s^{-1} is slow compared to the ionisation rate [28].

From the rotationally resolved part of spectra taken at different sensitivities a rotational temperature of $T_{rot} = (870 \pm 150)$ K can be deduced. Although this value should be taken with some caution since the low-J'' part is not resolved, a significant overpopulation of the low-J'' states as observed for desorption from NiO(1 1 1) [23] is not reflected in the spectra. For NiO(1 1 1) rotational temperatures of $T_{rot} = 200$ and 640 K have been observed [23]. The higher rotational excitation for the NiO(1 0 0) substrate supports the conclusion of a larger rotational corrugation in the excited state potential [29]. The spectra are taken at a delay time of 25 µs, corresponding to a velocity of 800 ms^{-1} for molecules desorbing in the direction of the surface normal. Although a significant rotation-translational coupling is observed, see below, a resulting correction of the rotational population lies well within the indicated uncertainty from different spectral scans. Also the above mentioned uncertainty due to unresolved low-J'' lines may account for a greater uncertainty in the average rotational energy.

The vibrational population can be estimated from the relative intensities of the B–X (0–0) and (1–1) bands. The Franck–Condon factors for the two transitions are nearly identical [30], and the ionisation cross-section can be assumed to be also the same due to the Rydberg character of the B state. In addition the photon energies to excite the two bands and thus ionise the B state differ only by about 30 cm^{-1}. Then from the spectra a vibrational population of about $N(v'' = 1) = 10\%$ can be deduced, corresponding to a vibrational temperature of $T_{vib} = 1340$ K. This vibrational temperature is within the experimental uncertainly identical to that observed for desorption from NiO(1 1 1) [23]. The population translates to an average vibrational energy of about $\langle E_{vib} \rangle = 214$ cm^{-1}. This value compares well with the average vibrational energy in the ($v'' = 1$) state of NO desorbing from NiO(1 0 0) using nanosecond [2] or femtosecond [5] laser pulses. Higher vibrationally excited states could not be observed, probably due to the high predissociation rate of B $^1\Sigma^+$($v' \geqslant 2$).

The main result of this letter concerns the velocity distribution of the desorbing CO molecules. For this purpose the probe laser pulse has been continuously delayed up to 220 µs with respect to the desorption laser pulse. At a flight distance of 20 mm this corresponds to a slow limit of 90 ms^{-1} velocity which has been recorded. This arrival time signal $S(t)$ has to be transformed first into a flight-time distribution $I(t)$ by

$$S(t) \propto \int_{v=L/t}^{v=(L+l)/t} I(v')dv' \approx I(v = L/t)\frac{l}{t} \qquad (2)$$

from which directly follows that

$$\Rightarrow I(v = l/t) \propto tS(t) \qquad (3)$$

where L denotes the flight distance, l the diameter of the probe laser and t is the arrival time.

Fig. 2 shows the results for various rotational states in $v'' = 0$. The individual velocity distributions are normalized
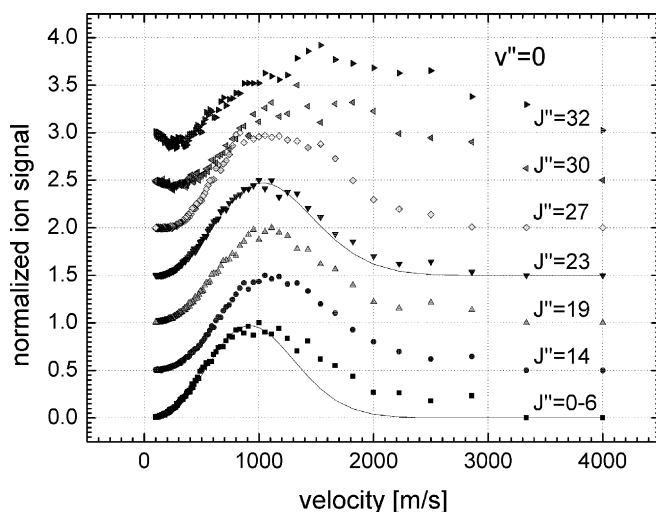

Fig. 2. Velocity distributions of CO ($v'' = 0$) desorbing in different rotational states. For $J'' = 0$–6 and $J'' = 23$ fits with Maxwellian flux distributions of $\langle E_{kin}/2k \rangle = 950$ K and 1200 K, respectively, are indicated.

to one at their maximum value and are displayed offset for clarity. For low to medium J'' the distributions are very similar and show a Maxwellian like velocity distribution. The maxima of the distributions appear around $1100 \, \mathrm{ms}^{-1}$. These distributions can approximately be described by kinetic temperatures between about $\langle E_{kin}/2k\rangle = 950$ K for $J'' = 0{-}6$ and 1200 K for $J'' = 23$. It is further evident that in addition to the Maxwellian distribution a component with velocities between 1500 and 3000 ms^{-1} is present. Beginning at $J'' = 27$ and pronounced at $J'' = 30$ and 32, this high velocity component gains in relative strength compared to the Maxwellian part mainly observed for the low-J'' molecules. Also the maximum of the distribution shifts to higher velocities around about 1500 ms^{-1}. Fig. 3 shows corresponding results for CO molecules desorbing in the vibrationally excited state, now for rotational states up to $J'' = 20$. For low J'' the distributions peak slightly below 1000 ms^{-1} and are approximately described by $\langle E_{kin}/2k\rangle = 1000$ to 1200 K. For higher J'' in $(v'' = 1)$, $J'' = 17$ and 20, the maximum shifts to about 1300 ms^{-1} and the best Maxwellian fits increase to 1400 and 1800 K, respectively. Again a fast velocity component increases in relative strength with increasing J''.

Fig. 4 shows the average kinetic energy of the states measured as a function of their rotational quantum number for CO molecules desorbing in both vibrational states. The average energy increases from about 250 meV at low J'' to more than 500 meV at $J'' = 30$. This increase is more monotonic for the vibrationally excited state while in the ground state the kinetic energy is approximately independent of J'' up to $J'' = 27$ with a significant increase at higher J''. It is therefore evident that a strong rotation–translation coupling is observed for CO desorption from NiO(100). Table 1 summarizes the average energies for CO and NO desorption from NiO(100) and NiO(111).
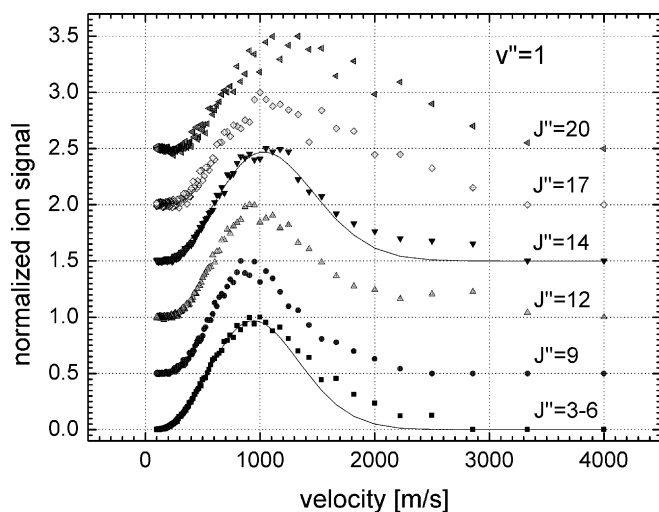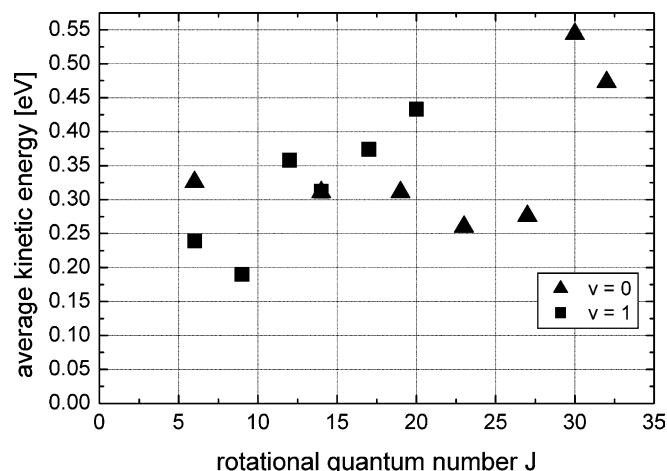

Fig. 4. Average kinetic energy $\langle E_{kin}\rangle$ of desorbing CO as a function of rotational quantum number; triangles: $(v'' = 0)$, squares: $(v'' = 1)$.

Table 1
Average energies for desorption from nickel oxide in $[\mathrm{cm}^{-1}]$

	CO		NO
	NiO(100)	NiO(111) [23]	NiO(100) [5]
$\langle E_{kin}\rangle$	2550	1600	1774
$\langle E_{rot}\rangle$	605	362	308
$\langle E_{vib}\rangle$	214[a]	236[a]	409

[a] For the vibrational energies the population in $(v'' = 1)$ only has been taken into account.

The observed velocity distributions differ significantly from those observed for the NiO(111) substrate [23]. There velocity distributions which can completely be described by Maxwellian flux distributions of $\langle E_{kin}/2k\rangle = (1150 \pm 150)$ K were found and a rotation–translation coupling could not be established up to $J'' = 23$. In the present study for the NiO(100) substrate the majority of the desorption flux up to medium J'' can also be described by a kinetic temperature of about 1000 to 1200 K. However, even at low J'' a fast component is present which increases in relative importance with J''. This also clearly indicates that the electronically excited state is rotationally more corrugated or has a significantly different equilibrium position in the angular coordinate than in the CO/NiO(111) system.

The observed velocity distributions are also very different from corresponding results for NO desorption from NiO(100) [3,5]. There, a clear bimodal distribution was observed with a slow component peaking around 300 ms^{-1} and a fast one around 1100 ms^{-1} at low J''. The distributions in this case were clearly non-Maxwellian, especially the fast one which displayed a nearly Gaussian distribution. This fast component showed a strong rotation–translation coupling, as in the present case for CO desorption.

Laser induced desorption of NO from metal surfaces is generally discussed in terms of a temporary formation of a NO^- state [1]. The dynamics then proceeds via an Anton-

Fig. 3. Same as Fig. 2 for CO $(v'' = 1)$. Maxwellian velocity distributions with $\langle E_{kin}/2k\rangle = 1000$ K for $J'' = 3{-}6$ and $\langle E_{kin}/2k\rangle = 1200$ K at $J'' = 14$ are shown as thin lines.

iewicz type mechanism [31], where this electronically excited state is more strongly bound to the surface with a shorter bond length than the ground state. For CO desorption from metal surfaces (Cu, Pt, Ru) [15–19] the unoccupied $2\pi^*$ level is of importance. After excitation with UV radiation electrons at the Fermi level of the metal can acquire sufficient energy to populate the antibonding hybride level in the Blyholder model. For near-IR radiation this is not longer the case. Beyond this one electron Blyholder model Jennison et al. [32] took correlation effects into account. In their adiabatic model the $2\pi^*$ level develops two antibonding levels, one energetically close to that of the Blyholder model and one at significantly lower energies. Loy and co-workers [33] conclude that this lower level can probably account for CO desorption by 800 nm radiation. This eventually leads to desorption of the CO molecule from metal surfaces.

For the desorption of NO from oxide surfaces direct charge transfer excitations seem to play an important role, as has been found theoretically [8–10] and is also confirmed experimentally for NiO as substrate [34]. For CO most experimental and theoretical information is available for $Cr_2O_3(0\,0\,0\,1)$ as substrate. Exciting this system with 6.4 eV radiation bimodal velocity distributions were observed for CO ($v'' = 0$) with one very slow component of only 300 ms^{-1} pointing towards a thermal origin of these molecules and a fast one with about 1300 ms^{-1}. For CO ($v'' = 1$) only a fast channel with velocities around 900 ms^{-1} appears [20]. For the electronic dynamics direct excitation of CO from the 5σ to the antibonding $2\pi^*$ state was considered in a 3D calculation [35]. A strong rotational corrugation of both potential energy surfaces was important to explain essential experimental results for the CO/$Cr_2O_3(0\,0\,0\,1)$ system. It seems conceivable that also for the CO/NiO(1 0 0) system a direct $5\sigma \rightarrow 2\pi^*$ excitation within the CO adsorbate constitutes the first excitation step. Whether the interaction of the excited electron with the substrate is strong enough to cause the development of two antibonding levels due to correlation effects, remains open. In the present experiment the energy of the exciting photon of 4.66 eV, however, is significantly lower than the gas phase $5\sigma \rightarrow 2\pi^*$ ($a^3\Pi$) transition energy, which is close to 6 eV. Since we observe a linear dependence of the desorption yield on the laser intensity and find a large desorption cross-section, the existence of an energetically lower antibonding level is corroborated.

In conclusion, the high rotational excitation supports the notion of a bent geometry for the electronically excited CO adsorbate. This is also corroborated by the observed rotation–translational coupling, which is a manifestation of a Franck–Condon excitation from the ground state at a different bond angle than the equilibrium geometry in the excited adsorbate. Further, the strong vibrational excitation of the desorbing molecules points to a bond length in the excited state different from the ground state.

References

[1] see, e.g. H.L. Dai, W. Ho (Eds.), Laser Spectroscopy and Photochemistry on Metal Surfaces, World Scientific, Singapore, 1995.
[2] Th. Mull, B. Baumeister, M. Menges, H.-J. Freund, D. Weide, C. Fischer, P. Andresen, J. Chem. Phys. 96 (1992) 7108.
[3] M. Menges, B. Baumeister, K. Al-Shamery, H.-J. Freund, C. Fischer, P. Andresen, J. Chem. Phys. 101 (1994) 3318.
[4] M. Wilde, O. Seifert, K. Al-Shamery, H.-J. Freund, J. Chem. Phys. 111 (1999) 1158.
[5] G. Eichhorn, M. Richter, K. Al-Shamery, H. Zacharias, J. Chem. Phys. 111 (1999) 386.
[6] H. Kuhlenbeck, G. Odörfer, R. Jaeger, G. Illing, M. Menges, Th. Mull, H.-J. Freund, M. Pöhlchen, V. Staemmler, S. Witzel, C. Scharfschwerdt, K. Wennemann, T. Liedke, M. Neumann, Phys. Rev. B 43 (1991) 1969.
[7] J.T. Hoeft, M. Kittel, M. Polcik, S. Bao, R.L. Toomes, J.H. Kang, D.P. Woodruff, M. Pascal, C.L.A. Lamont, Phys. Rev. Lett. 87 (2001) 086101.
[8] T. Klüner, H.-J. Freund, F. Freitag, V. Staemmler, J. Chem. Phys. 104 (1996) 10030.
[9] T. Klüner, H.-J. Freund, V. Staemmler, R. Kosloff, Phys. Rev. Lett. 80 (1998) 5208.
[10] C.P. Koch, T. Klüner, H.-J. Freund, R. Kosloff, J. Chem. Phys. 119 (2003) 1750.
[11] D. Cappus, J. Klinkmann, H. Kuhlenbeck, H.-J. Freund, Surf. Sci. 325 (1995) L 421.
[12] M. Kittel, J.T. Hoeft, S. Bao, M. Polcik, R.L. Toomes, J.H. Kang, D.P. Woodruff, M. Pascal, C.L.A. Lamont, Surf. Sci. 499 (2002) 1.
[13] G. Pacchioni, C. Di Valentin, D. Dominguez-Ariza, F. Illas, T. Bredow, T. Klüner, V. Staemmler, J. Phys. Condens. Mater. 16 (2004) S2497.
[14] A. Rohrbach, J. Hafner, G. Kresse, Phys. Rev. B 69 (2004) 075413.
[15] L.M. Struck, L.J. Richter, S.A. Buntin, R.R. Cavanagh, J.C. Stephenson, Phys. Rev. Lett. 77 (1996) 4576.
[16] F.-J. Kao, D.G. Busch, D. Gomes da Costa, W. Ho, Phys. Rev. Lett. 70 (1993) 4098.
[17] S. Deliwala, R.J. Finlay, J.R. Goldman, T.H. Her, W.D. Mieher, E. Mazur, Chem. Phys. Lett. 242 (1995) 617.
[18] S. Funk, M. Bonn, D.N. Denzler, Ch. Hess, M. Wolf, G. Ertl, J. Chem. Phys. 112 (2000) 9888.
[19] L. Cai, X. Xiao, M.M.T. Loy, Surf. Sci. 464 (2000) L 727.
[20] K. Al-Shamery, I. Beauport, H.-J. Freund, H. Zacharias, Chem. Phys. Lett. 222 (1994) 107.
[21] I. Beauport, K. Al-Shamery, H.-J. Freund, Chem. Phys. Lett. 256 (1996) 641.
[22] S. Borowski, T. Klüner, H.-J. Freund, I. Klinkmann, K. Al-Shamery, M. Pykavy, V. Staemmler, Appl. Phys. A 78 (2004) 223.
[23] M. Asscher, F.M. Zimmermann, L.L. Springsteen, P.L. Houston, W. Ho, J. Chem. Phys. 96 (1992) 4808.
[24] R. Wichtendahl, M. Rodriguez-Rodrigo, U. Härtel, H. Kuhlenbeck, H.-J. Freund, Surf. Sci. 423 (1999) 90.
[25] G.W. Loge, J.J. Tiee, F.B. Wampler, J. Chem. Phys. 79 (1983) 196.
[26] J.B. Halpern, H. Zacharias, R. Wallenstein, J. Mol. Spectrosc. 79 (1980) 1.
[27] S.G. Tilford, J.T. Vanderslice, J. Mol. Spectrosc. 26 (1968) 419.
[28] H. Rottke, H. Zacharias, Opt. Commun. 55 (1985) 87.
[29] E. Hasselbrink, Chem. Phys. Lett. 170 (1990) 329.
[30] T.A. Carlson, N. Duric, P. Erman, M. Larsson, Z. Phys. A 287 (1978) 123.
[31] P.R. Antoniewicz, Phys. Rev. B 21 (1980) 3811.
[32] D.R. Jennison, E.B. Stechel, A.R. Burns, J. Electr. Spectr. Rel. Phen. 72 (1995) 9.
[33] L. Cai, X. Xiao, M.M.T. Loy, Surf. Sci. 492 (2001) L 688.
[34] H. Zacharias, G. Eichhorn, R. Schliesing, K. Al-Shamery, Appl. Phys. B 68 (1999) 605.
[35] S. Thiel, M. Pykavy, T. Klüner, H.-J. Freund, R. Kosloff, V. Staemmler, J. Chem. Phys. 116 (2002) 762.